Results from the N^* Program at JLab

I. Aznauryan[1,2]**, V.D. Burkert**[1]**, T.-S. H. Lee**[3,4]**, V. Mokeev**[1,5]

[1]Thomas Jefferson National Accelerator Facility, Newport News, Virginia 23606, USA

[2] Yerevan Physics Institute, Yerevan 375036, Armenia

[3]Physics Division, Argonne National Laboratory, Argonne, Illinois 60439, USA

[4] Excited Baryon Analysis Center, Thomas Jefferson National Accelerator Facility, Newport News, Virginia 23606, USA

[5] Skobeltsyn Nuclear Physics Institute at Moscow State University, 119899, Moscow, Russia

E-mail: `aznaury@jlab.org`, `burkert@jlab.org`, `lee@phy.anl.gov`, `mokeev@jlab.org`

Abstract. We discuss the results on the fundamental degrees of freedom underlying the nucleon excitation spectrum and how they evolve as the resonance transitions are investigated with increasingly better space-time resolution of the electromagnetic probe. Improved photocouplings for a number of resonant states, those for the $N(1720)P_{13}$ being significantly changed, have been determined and entered into the 2008 edition of the RPP. Strong sensitivity to the $N(1900)P_{13}$ state, that is listed now as a 2-star state in the same edition of RPP, has been observed in $K\Lambda$, $K\Sigma$ photoproduction. None of the earlier observations of a $\Theta_5^+(1540)$ was confirmed in a series of three JLab high statistics dedicated measurements, and stringent upper limits on production cross sections were placed in several channels. For the four lowest excited states, the $\Delta(1232)P_{33}$, $N(1440)P_{11}$, $N(1520)D_{13}$, and $N(1535)S_{11}$, the transition amplitudes have been measured in a wide range in photon virtuality Q^2. The amplitudes for the Δ show the importance of the pion-cloud contribution and don't show any sign of approaching the pQCD regime for $Q^2 < 7$ GeV^2. For the Roper resonance, $N(1440)P_{11}$, the data provide strong evidence for this state as a predominantly radial excitation of the nucleon as a 3-quark ground state. For the $N(1535)S_{11}$, comparison of the results extracted from π and η photo- and electroproduction data allowed one to specify the branching ratios of this state to the πN and ηN channels; they will enter into the 2010 edition of the RPP. Measured for the first time, the longitudinal transition amplitude for the $N(1535)S_{11}$ became a challenge for quark models and can be indicative of large meson-cloud contributions or alternative representations of this state. The $N(1520)D_{13}$ clearly shows the rapid changeover from helicity-3/2 dominance at the real photon point to helicity-1/2 dominance at $Q^2 > 0.5$ GeV^2, confirming a long-standing prediction of the constituent quark model. The search for undiscovered but predicted states continues to be pursued with a vigorous experimental program. While recent data from JLab and elsewhere provide intriguing hints of new states, final conclusions will have to wait for the results of the broad experimental effort currently underway with CLAS, and subsequent analyses involving the EBAC at JLab.

1. Introduction

Over 98% of the mass of the visible universe is made of nucleons. They are at the core of atoms and nuclei in stars that provide the energy that heat the planets and allows for life to exist on at least one of them, our earth. Understanding their internal structure has been at the center of nuclear and particle physics for decades. Similar to atomic nuclei, nucleons are complex systems of confined quarks and gluons and exhibit characteristic spectra of excited states that

encode information on symmetry properties of baryonic matter. Highly excited nucleon states (N^*) are sensitive to details of quark confinement, which is poorly understood within Quantum Chromodynamics (QCD), the fundamental theory of strong interactions. Measurements of excited nucleon states are needed to come to a better understanding of how confinement works in nucleons. The clustering of quarks in the nucleon can lead to an excitation spectrum with fewer states than if quarks do not cluster. The N^* states couple strongly to the meson-baryon continuum to form nucleon resonances of characteristic masses and decay widths, and can be most effectively investigated by using meson production reactions on the nucleon. With the high precision electron beam and the CEBAF Large Acceptance Spectrometer (CLAS) in Hall B, Jefferson Laboratory (JLab) has developed an excited baryon program and has made important contributions in this direction.

The excited baryon program at JLab has two main objectives. The first one is to provide information from electromagnetic probes to improve our understanding of the systematics of the N^* spectrum and the nature of the effective degrees of freedom in low energy QCD. The second objective is to measure the resonance transition form factors from the nucleon ground state to the excited baryon states. These measurements probe the internal structure of excited states and provide information about the confining forces of the 3-quark system and the spatial distribution of quarks in the transverse plane.

The experimental program makes wide use of the CLAS detector [1], which is depicted in Fig. 1. CLAS provides particle detection and identification, as well as momentum analysis in a polar angle range from $8°$ to $140°$. For operation of energy-tagged photon beams, the photon energy tagging facility provides photons with an energy resolution of $\frac{\sigma(E)}{E} = 10^{-3}$, and covers an energy range from 20% to 95% of the incident electron beam energy. Other equipment essential for the N^* program includes the coherent bremsstrahlung facility that has been used to produce linearly polarized photons with polarizations up to 90%. There are also two frozen-spin polarized targets, one using butanol as target material for polarized protons (FROST), and the other using HD as an efficient neutron target (HD-Ice). FROST has been operated successfully in longitudinal polarization mode, in conjunction with linearly and circularly polarized photons, and is planned to be used in transverse polarization mode in 2010. HD-Ice is planned to be used as a polarized neutron target in 2010/2011. In addition, the highly polarized electron beam, $P_e = 0.85$, generates circularly polarized photons when scattered off an amorphous radiator. The polarization transfer is maximum at the highest photon energies.

CLAS is also being employed for the measurement of electroproduction of single and double pions, and other pseudoscalar mesons, e.g. K^+, K^-, K_s^0. Some of these experiments make use of a dynamically polarized nucleon target [2]. Some experiments, focusing on specific kinematics, make use of the magnetic spectrometer setups in Hall A, using proton recoil polarimeters for the measurement of single and double polarization observables, and in Hall C to study high Q^2 pion and eta production. The list of experiments approved to study N^* excitations or search for new states is given in Table 1.

In addition to analyzing the electromagnetic meson production data, it is important to interpret the extracted N^* parameters in terms of QCD. The Excited Baryon Analysis Center (EBAC) was established at JLab in 2006 to address this problem. This effort is making rapid progress by making a dynamical coupled-channels analysis of the world data of both the hadronic and electromagnetic meson production data. In addition, effort has been made to make contact with hadron structure calculations, in particular the LQCD effort at JLab.

In Sections 2 and 3, the results from analyzing the JLab photoproduction and electroproduction data will be described. The progress and status of EBAC will be given in Section 4. Section 5 is devoted to the discussion of the future prospects of the N^* program at 6 GeV and of the possibilities with the 12-GeV upgrade.
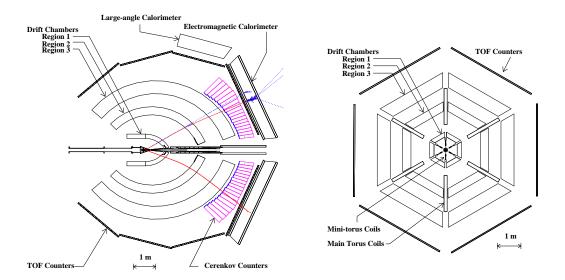
Figure 1. The CEBAF Large Acceptance Spectrometer (CLAS). A cut along the beamline (with the beam incident from the left) is shown on the l.h.s., while the r.h.s. shows a cut perpendicular to the beam. A superconducting toroidal magnet provides the magnetic analysis in six independent sectors. Each of the six sectors is independently instrumented with tracking chambers and with detectors for particle identification.

$p(\gamma, K)X$	[3]	$p(e, e'K^+K^-)p, p(e, e'K^+\pi^-)X$	[17]
$p(\gamma, \eta, \eta')p$	[4]	$p(e, e'\pi)N$	[18]
$D(\gamma, \eta), \ D(\gamma, \eta')$	[5]	$\vec{p}(\vec{e}, e'p)\pi^0$	[19]
$p(\gamma, \pi)N$	[6]	$p(e, e'\omega)p$	[20]
$p(\vec{\gamma}, \omega)p$	[7]	$p(e, e'\pi^+\pi^-)p$	[21]
$\vec{\gamma}\vec{p} \to K^+\Lambda, K^+\Sigma, K^0\Sigma^+$	[8]	$\vec{p}(\vec{e}, e'\pi)n$	[22]
$\vec{p}(\vec{\gamma}, \pi^+)n, \vec{p}(\vec{\gamma}, p)\pi^0$	[9]	$p(\vec{e}, e'p)\pi^0, \ p(\vec{e}, e'\pi^+)n$	[23]
$\vec{p}(\vec{\gamma}, \eta)p$	[10]	$p(e, e'p)\pi^0$	[24]
$\vec{p}(\vec{\gamma}, \pi^+\pi^- p)$	[11]	$p(e, e'K^+)\Lambda, \Sigma$	[25]
$n(\vec{\gamma}, K\Lambda)$	[12]	$p(e, e'\pi^0)p, p(e, e'\pi^+)n$	[26]
$p(e, e'\pi)N$	[13]	$p(e, e'\pi^+\pi^- p)$	[27]
$p(e, e'\pi^+)n, \ p(e, e'p)\pi^0, \ n(e, e'\pi^-)p$	[14]	$p(\vec{e}, e'K, \vec{\Lambda}, \vec{\Sigma})$	[28]
$p(e, e'p)\eta$	[15]	$p(e, e'p)\pi^0, \eta$	[29]
$p(\vec{e}, e'p)\pi^0, \ p(\vec{e}, e'\pi^+)n$	[16]		

Table 1. Experiments at JLab that are part of the N^* program.

2. Results from Photoproduction Experiments

2.1. Photoproduction of pseudoscalar mesons

Precise differential cross sections on proton targets for final states $p\pi^0$ [30], $n\pi^+$ [31], $p\eta$ [32], $p\eta'$ [33], $K^+\Lambda$ [34, 35], and $K^+\Sigma^0$ [34, 35] have been measured. As an example, Fig. 2 shows differential cross sections for $\gamma p \to n\pi^+$ for different hadronic mass W. These data, together with the $\pi N \to \pi N$ elastic data and the cross sections from the $\gamma p \to p\pi^0$ channel also measured
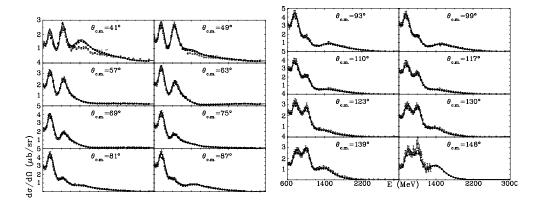
Figure 2. Differential cross sections from CLAS for $\gamma p \rightarrow n\pi^+$ [31] vs. photon energy E ($W^2 = m_p^2 + 2m_p E$). Solid and open circles show, respectively, the CLAS and previous data. New measurements [31] have improved the world data base significantly in energy range and polar angle coverage. Curves show the results of the SAID FA08 solution.

with CLAS, have been used to determine improved helicity amplitudes for a number of resonant states with significant couplings to the single pion channel. They have been also entered into the 2008 edition of the Review of Particle Physics (RPP) [36]. For example, the photocoupling of the N(1720)P$_{13}$ has changed significantly with the new precise data. More complex processes such as $\gamma p \rightarrow p\pi^+\pi^-$ are also being studied. The latter are particularly sensitive to higher-mass nucleon resonances that couple dominantly to the $\Delta\pi$ or $N\rho$ isobars with two pions in the final state.

In photoproduction of single pions or etas, partial wave analyses of differential cross sections alone result in ambiguous solutions for the contributing resonant partial waves. The CLAS N^* program is therefore aimed at complete or nearly complete measurements for all of these processes. Complete information may be obtained using a combination of linearly and circularly polarized photon beams, measurement of the hyperon recoil polarization, and using longitudinally and transversely polarized targets. Single pseudoscalar meson production is fully described by 4 complex, parity conserving amplitudes, requiring eight [37] well-chosen combinations of beam, target, and recoil polarization measurements for an unambiguous extraction of the production amplitude. Table 2 shows the observables that can be determined from these measurements. If all possible combinations are measured, 16 observables can be extracted. In measurements that involve nucleons in the final state with no recoil polarization being measured, 7 independent observables can be measured directly. In addition, the recoil polarization asymmetry P can be inferred from the double polarization asymmetry with a linearly polarized beam and transverse target polarization.

In addition to precise $K\Lambda$ and $K\Sigma$ cross section data, recoil polarization and polarization transfer data have been measured [38]. The recoil polarization data in the $K^+\Lambda$ sector showed a highly unexpected behavior: the spin transfer from the circularly polarized photon to the Λ hyperon is complete, creating the Λ hyperon 100% polarized, as can be seen in Fig. 3. The sum of all polarization components $R^2 \equiv P^2 + C_x^2 + C_z^2$, which has an upper bound of 1, is consistent with $R^2 = 1$ throughout the region covered by the measurement. The combined analysis of the CLAS cross section and polarization transfer data by the Bonn-Gatchina group [39] shows strong sensitivity to a N(1900)P$_{13}$ candidate state. The decisive ingredient in this analysis was the CLAS spin transfer data. An N(1900)P$_{13}$ state is listed as a 2-star candidate state in the 2008 edition of the RPP [36]. If this assignment is further corroborated, the existence of an N(1900)P$_{13}$ state will provide strong evidence against the quark-diquark model that has no place for such a state in this mass range [40].
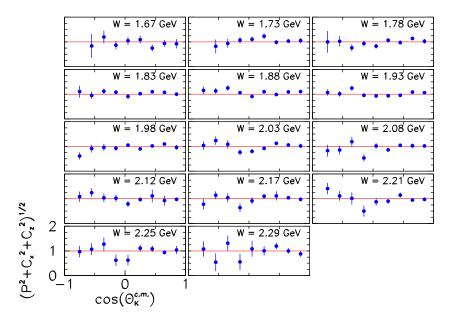
Figure 3. CLAS data [38] on the polarization observable vector combining recoil polarization P and transferred polarization components C_x and C_z for the Λ hyperons produced in $\vec{\gamma} + p \rightarrow K^+ + \vec{\Lambda}$. Lower-left axis scales apply to all plots. The data show the Λ is 100% polarized. These data were crucial when fitted simultaneously with the CLAS $K^+\Lambda$ and $K^+\Sigma$ differential cross section data. They provided evidence for an N(1900)P$_{13}$ candidate state, which is required for a good simultaneous fit to the cross section and spin transfer data.

New precise high statistics data with a linearly polarized photon beam on a proton target are becoming also available. Preliminary results for the process $\vec{\gamma}p \rightarrow K^+\Lambda$ in just one energy bin are shown in Fig. 4. For the partial wave analysis, complete angle coverage in all observables is especially important.

2.2. Search for new cascade (Ξ) baryons

The production of Ξ baryons, i.e. strangeness $S = -2$ excited states, provides another promising way of searching for new baryon states due to the expected narrower widths of these states compared to $S = 0$ and $S = -1$ resonances. However, the disadvantage of using a photon beam for detection of the $S = -2$ states is that they require production of at least two kaons in the final state. Possible production mechanisms include t-channel K or K^* exchanges on proton targets with an excited hyperon Y^* (Λ^* or Σ^*) as an intermediate state and with subsequent decays $Y^* \rightarrow K^+ + \Xi^*$ and $\Xi^* \rightarrow \Xi\pi$ or $\Xi \rightarrow \Lambda(\Sigma)\bar{K}$. The missing mass technique may work for $\gamma p \rightarrow K^+K^+X$ if the state is sufficiently narrow to be observed as a peak in the missing mass spectrum. Fig. 5 shows that one can identify the lowest two cascade states in this way. To identify the higher-mass states, higher energies are needed.

Another possibility to isolate excited cascade baryons is to measure additional particles in the final state resulting from the decays of the excited Ξ, e.g. $K^+K^+\Xi^0\pi^-$. The invariant mass of the $\Xi\pi^-$ system shows the first exited state $\Xi(1530)$ and indications of additional structure near 1620 MeV. A state near that mass is predicted as a dynamically generated $\Xi\pi$ system in
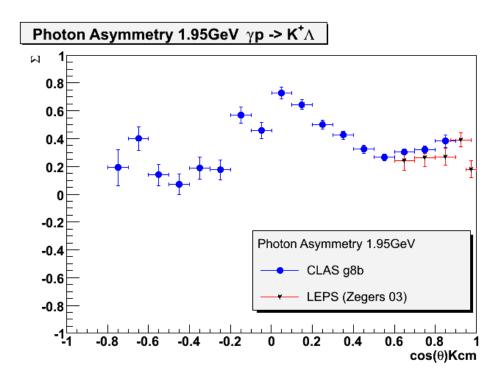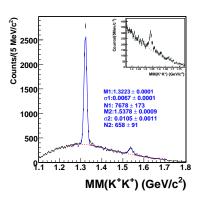
Photon Asymmetry 1.95GeV $\gamma p \to K^+\Lambda$

Photon Asymmetry 1.95GeV
- CLAS g8b
- LEPS (Zegers 03)

Figure 4. Beam asymmetry for $\vec{\gamma}p \to K^+\Lambda$ with linearly polarized photons. Preliminary CLAS data are shown for $W = 1.95$ GeV. The previous data are from GRAAL [41] and LEPS [42].

Photon	T			R			T			-			R		
				x'	y'	z'	x	y	z	x	y	z	x	y	z
	x	y	z				x	y	z	x	y	z	x	y	z
I		T			P		$T_{x'}$			$L_{x'}$		Σ	$T_{z'}$			$L_{z'}$
II	H	P	G	$O_{x'}$	T	$O_{z'}$	$L_{z'}$	$C_{z'}$	$T_{z'}$	E		F	$L_{x'}$	$C_{x'}$	$T_{x'}$	
III	F		E	$C_{x'}$		$C_{z'}$			$O_{z'}$		G	H		$O_{x'}$		

Table 2. Polarization observables in $J^\pi = 0^-$ meson photoproduction that can be extracted from complete experiments using all combinations of beam, target, and recoil polarizations. I,II,III correspond, respectively, to unpolarized, linearly and circularly polarized photon beams. The observables given in black letters are directly extractable. Other observables provide additional redundant information: green letters show the single-polarization observables measured from double-polarization asymmetries, blue letters show the double-polarization observables measured from triple-polarization asymmetries. For example, the target polarization asymmetry T can be extracted in a single-polarization measurement with unpolarized beam and a transversely polarized target, and also in a double-polarization measurement with a linearly polarized beam and measurement of the recoil polarization $P_{y'}$. This allows multiple cross checks of measurements with different systematics.

the model of Ref. [43]. The data have insufficient statistics and were taken at too low of an energy to allow further investigations. New data taken at 5.5 GeV electron energy and with higher statistics are currently being analyzed, and should allow more definite conclusions.
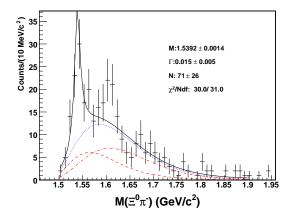
Figure 5. Missing mass spectrum M_X for $\gamma p \to K^+ K^+ X$. The Ξ ground state and first excited state are clearly identified. The right panel shows the invariant mass of $\Xi^0(1320)\pi^-$. The low mass peak is the $\Xi(1530)$. The other structure near 1620 MeV is statistically not significant.

2.3. Demise of the pentaquarks?

In 2003 and 2004, about a dozen experiments in nuclear physics and high energy physics laboratories claimed the observation of several states with flavor exotic quantum numbers, $\Theta_5^+(1540)$, $\Phi_5(1860)$, and $\Theta_c^0(3100)$. For a summary see Ref. [44]. These claims were exclusively based on non-dedicated experimental observations. At JLab a series of three high statistics dedicated measurements was conducted in 2004 and 2005 with CLAS to verify some of these claims. None of the earlier observations of a $\Theta_5^+(1540)$ could be confirmed and stringent upper limits on production cross sections were placed in several channels, in particular, $\gamma p \to \bar{K}^0 K^0$, $\bar{K}^0 K^+ n$ [45, 46], $\gamma n \to K^- K^+ n$ [47], $\gamma D \to \Lambda n K^+$ [48], $\gamma p \to K^+ K^- p$ [49]. Other channels are still being evaluated.

3. Results from Electroproduction Experiments

3.1. JLab/CLAS data on single pion electroproduction

The CLAS detector at Jefferson Lab is the first full acceptance instrument designed for the comprehensive investigation of exclusive electroproduction of mesons with the goal to study the electroexcitation of nucleon resonances in detail. In recent years, a variety of measurements of single pion electroproduction on protons have been performed at CLAS in a wide range of Q^2 from 0.16 to 6 GeV^2 [50]-[57]. The obtained experimental data include about 119,000 data points of differential cross sections, longitudinally polarized beam asymmetries, and longitudinal target and beam-target asymmetries. A comprehensive analysis of these data was performed using two approaches: one, based on fixed-t dispersion relations (DR), and another, based on the effective Lagrangian approach - Unitary Isobar Model (UIM).

The DR approach was developed for pion photo- and electroproduction on nucleons in the 50s [58, 59] and played an extremely fruitful role in the analyses of the data for these processes. In recent publications [60, 61, 62, 63], this approach was further developed by extending it into the wide kinematical region in W and Q^2 covered by the new data. DR allowed also to obtain strict constraints on the multipole amplitudes $M_{1+}^{3/2}$, $E_{1+}^{3/2}$, $S_{1+}^{3/2}$ that correspond to the contribution of the prominent $\Delta(1232)\mathrm{P}_{33}$ resonance [61]. The constraint on the large $M_{1+}^{3/2}$ amplitude plays an important role in the reliable extraction of the amplitudes for the $\gamma^* N \to \Delta(1232)\mathrm{P}_{33}$ transition. It also impacts the analysis of the second resonance region, because resonances from this region are overlapping with the $\Delta(1232)\mathrm{P}_{33}$.
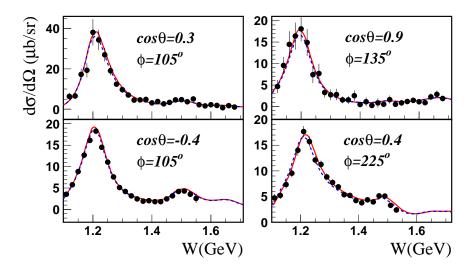
Figure 6. W-dependence of the differential cross sections for $\gamma^*p \to \pi^0 p$ (upper row) and $\gamma^*p \to \pi^+ n$ (lower row) at $Q^2 = 0.4$ GeV^2 for different polar and azimuthal angles. Data are from Refs. [50] (π^0) and [53] (π^+). The solid (dashed) curves correspond to the results obtained using the DR (UIM) approach [63].

Starting in the late 90s, another approach, the UIM [64] (also known as MAID), became widely used for the analyses of single-pion photo- and electroproduction data. This approach was modified in Ref. [61] by the incorporation of Regge poles, which enabled a good description of all photoproduction multipole amplitudes up to an invariant mass $W = 2$ GeV using a unified Breit-Wigner parametrization of the resonance contributions.

Within DR and UIM, the analyses of the data [50]-[57] were performed in Refs. [62, 63, 65, 66]. As a result, the helicity amplitudes for the electroexcitation of the low mass resonances $\Delta(1232)P_{33}$, N(1440)P$_{11}$, N(1520)D$_{13}$, and N(1535)S$_{11}$ were extracted from the experimental data in a range of Q^2 up to 6 GeV^2. The non-resonant contributions are built in DR and UIM in conceptually different ways; this allowed to draw conclusions on the model sensitivity of the resulting electroexcitation amplitudes. Model uncertainties caused by the higher-mass resonances and by the non-resonant amplitudes due to the uncertainties in the Born terms (the s- and u-channel nucleon exchanges and t-channel pion contribution) and in the ρ and ω t-channel contributions were also evaluated. All uncertainties were added in quadrature and presented as model uncertainties of the extracted electroexcitation amplitudes.

In Figs. 6-10, some examples that show the description of the data are presented. Shown are the W-dependences of the differential cross sections for different reactions at several Q^2, polar and azimuthal angles. The W-dependences of σ_{tot}, $\sigma_{tot}^{LT'}$, and of the target (A_t) and beam-target (A_{et}) asymmetries for $\vec{e}\vec{p} \to ep\pi^0$ integrated over cosθ, ϕ and Q^2 are also shown.

3.2. JLab/CLAS data on two pion electroproduction

Two pion electroproduction is one of the biggest contributors to the N^* electroexcitation. This exclusive channel is sensitive to almost all well established excited states and in particular to high lying resonances with masses above 1.6 GeV. According to the quark model expectations [67, 68], two pion electroproduction has a great potential for the discovery of the so-called "missing" baryon states.

A combination of the CEBAF continuous electron beam and detector CLAS for the first time makes it possible to measure nine independent one-fold differential $\gamma^*p \to \pi^+\pi^- p$ cross sections,
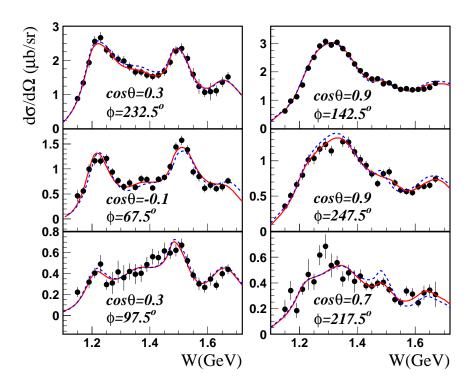
Figure 7. W-dependence of the differential cross section for $\gamma^* p \to \pi^+ n$ for different polar and azimuthal angles. Upper, middle, and lower rows are for $Q^2=1.72$, 2.44, 3.48 GeV^2, respectively. Data are from Ref. [56]. Other notations as in Fig. 6.
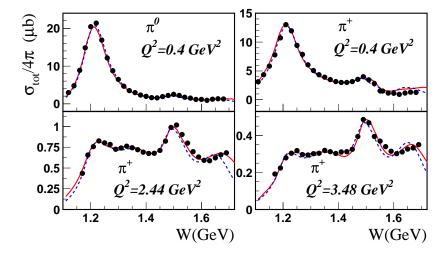

Figure 8. W-dependence of the $\gamma^* p \to \pi^0 p, \pi^+ n$ total cross sections. Data are from Refs. [50, 53, 56]. Other notations as in Fig. 6.
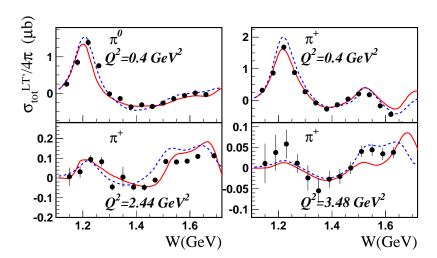
Figure 9. W-dependence of the structure function $\sigma_{tot}^{LT'}$ corresponding to a longitudinally polarized electron beam integrated over polar angle. Data are from Refs. [51, 52, 56]. Other notations as in Fig. 6.
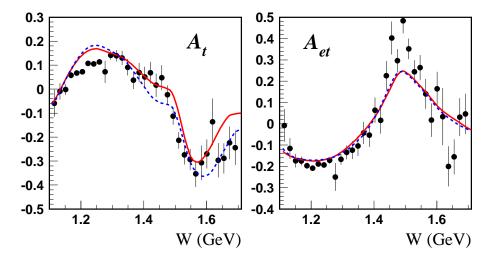

Figure 10. W-dependence of the target (A_t) and beam-target (A_{et}) asymmetries for $\vec{e}\vec{p} \to ep\pi^0$ integrated over $\cos\theta$, ϕ and Q^2 ($0.252 < Q^2 < 0.611$ GeV^2). Data are from Ref. [57]. Other notations as in Fig. 6.

as well fully integrated cross sections, in the kinematical areas presented in Table 3. The high statistics and good momentum resolutions of the measurements allowed to use bin sizes of W and Q^2, which are several times smaller than the ones used in previous measurements.

All essential mechanisms contributing to $\pi^+\pi^-p$ electroproduction were established from the analysis of these data within the framework of the reaction model presented in Ref. [71]. This model provides good data description, allowing to isolate resonant contributions to observables, needed for evaluation of γ^*NN^* electrocouplings.

The CLAS data [70] for the first time revealed the structure in the fully integrated $\pi^+\pi^-p$ electroproduction cross sections at $W \approx 1.7\,GeV$, shown in Fig. 11. Analysis of these data within the framework of the reaction model [71] offers an evidence for the candidate state $3/2^+(1720)$. Signals from this possible new state can be seen in Fig. 11. If these signals will be confirmed in

Q^2 coverage , GeV^2	W coverage, GeV	Bin size over W/Q^2 , GeV/GeV^2	Data status
0.20-0.60	1.30-1.57	0.025/0.050	Completed [69]
0.50-1.50	1.40-2.10	0.025/0.3-0.4	Completed [70]
2.0-5.0	1.40-2.00	0.025/0.5	In progress
0.	1.60-2.80	0.025	In progress

Table 3. Kinematical areas covered by the CLAS measurements of the $\pi^+\pi^-p$ photo- and electroproduction cross sections.
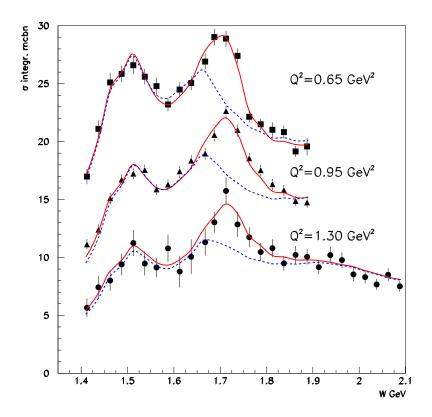

Figure 11. Description of the CLAS data [70] on fully integrated $\pi^+\pi^-p$ electroproduction cross sections within the framework of the reaction model [71] with parameters fitted to one-fold differential cross sections. The calculations, taking into account the contributions from the conventional N^*'s only, are shown by the dashed lines, while the solid lines correspond to the fit after implementation of the $3/2^+(1720)$ candidate state. Difference between solid and dashed lines represents a signal from the possible new state.

the future combined analysis of the CLAS $\pi^+\pi^-p$ photo- and electroproduction data (Table 3), we would obtain an unambiguous evidence for long awaited "missing" baryon state.

Evaluation of γ^*NN^* electrocouplings from the CLAS $\pi^+\pi^-p$ electroproduction data is in progress. The γ^*NN^* electrocouplings for almost all N^* states will be determined at photon virtualities $Q^2 < 5.0\,\mathrm{GeV}^2$. Preliminary results may be found in Refs. [72, 73]. Single and charge double pion electroproduction channels have completely different non-resonant contributions and provide independent information on the extracted resonance electrocouplings. The consistent results obtained from analyses of the dominant πN and $\pi^+\pi^-p$ exclusive channels will offer an evidence for reliable extraction of these fundamental quantities from the meson electroproduction data.

Finally, we are planning a combined analysis of single and charge double pion electroproduction data within the framework of advanced coupled-channel approach, that is described in Sec. 4.

3.3. Other JLab data on exclusive meson electroproduction

There are JLab Hall A and Hall C measurements of π^0 electroproduction on the proton in the $\Delta(1232)\mathrm{P}_{33}$ resonance region that include Hall A data on recoil polarization response functions at $Q^2 = 1\,\mathrm{GeV}^2$ [74, 75] and Hall C data on differential cross sections at $Q^2 = 2.8,\ 4.2\,\mathrm{GeV}^2$ [76] and 6.4, 7.7 GeV^2 [77]. Measurements of η electroproduction on the proton were performed in Hall B with CLAS and in Hall C; they include CLAS data at $Q^2 = 0.165 - 3.1\,\mathrm{GeV}^2$ [78, 79] and Hall C data at $Q^2 = 2.4,\ 3.6\,\mathrm{GeV}^2$ [80], $Q^2 = 5.7,\ 7\,\mathrm{GeV}^2$ [81].

3.4. The $\Delta(1232)\mathrm{P}_{33}$ resonance

The excitation of the $\Delta(1232)\mathrm{P}_{33}$ has been studied for more than 50 years with various probes. But only in the past decade have the experimental tools become available in electron scattering to enable precise measurements in exclusive π production from protons with photon virtualities up to $Q^2 = 8\,\mathrm{GeV}^2$. Benchmark results from CLAS and other laboratories are shown in Fig. 12. New exclusive measurements confirm a rapid falloff of the $\gamma^*p \to \Delta(1232)\mathrm{P}_{33}$ magnetic-dipole form factor relative to that for the proton seen previously in inclusive experiments. There has been a long-standing underestimation of the data for this form factor by the constituent quark model. Within dynamical reaction models [86, 89, 90], the pion-cloud contribution was identified as the source of this discrepancy. The importance of the pion-cloud contribution for the $\gamma^*p \to \Delta(1232)\mathrm{P}_{33}$ transition is confirmed also by the lattice QCD calculations [91]. In Fig. 12, the results of the dynamical model [86] are given that show that the pion-cloud contribution makes up more than 30% of $G_M^*(Q^2)$ at the photon point, and remains sizeable at the highest Q^2.

The Q^2-dependence of R_{EM} and R_{SM} is of great interest as a measure of the Q^2 scale where the approach to the asymptotic domain of QCD may set in. In the pQCD asymptotics $R_{EM} \to 1$ and $R_{SM} \to const$. The data on R_{EM}, R_{SM} show that in the range $Q^2 < 7\,\mathrm{GeV}^2$, there is no sign of an approach to the asymptotic pQCD regime in either of these ratios.

3.5. The Roper resonance $N(1440)\mathrm{P}_{11}$ - a puzzle resolved

By quantum numbers, the simplest and most natural classification of the Roper resonance in the constituent quark model is as a first radial excitation of the $3q$ ground state. However, difficulties of quark models to describe the low mass and large width of the $N(1440)\mathrm{P}_{11}$, and also its electroexcitation amplitudes on proton and neutron at the photon point, gave rise to numerous speculations around this state. Alternative descriptions of this state as a gluonic baryon excitation [92, 93], or as a hadronic $N\sigma$ molecule [94], were suggested. The CLAS measurements, for the first time, allowed the determination of the electroexcitation amplitudes of the Roper resonance on the proton in the range $Q^2 < 4.5\,\mathrm{GeV}^2$ (Fig. 13). These results are
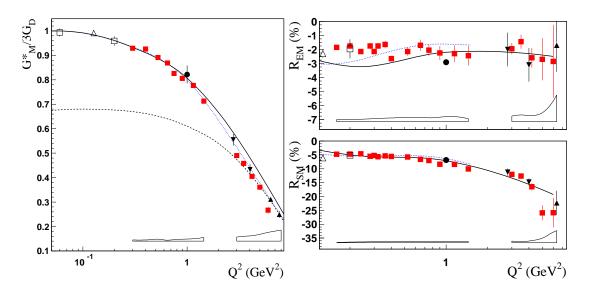
Figure 12. Left panel: the form factor G_M^* [82] for the $\gamma^* p \to \Delta(1232)P_{33}$ transition relative to $3G_D(Q^2)$: $G_D(Q^2) = 1/(1 + \frac{Q^2}{0.71 \ GeV^2})$. Right panel: the ratios $R_{EM} \equiv E_{1+}^{3/2}/M_{1+}^{3/2}$, $R_{SM} \equiv S_{1+}^{3/2}/M_{1+}^{3/2}$. The solid boxes are the results extracted from the CLAS data [50, 51, 54, 55] in Ref. [63]. The bands show the model uncertainties of the results. Also shown are the results from JLab/Hall A [74, 75] - solid circles and JLab/Hall C [76, 77] - solid triangles. The low Q^2 results are from MAMI [83, 84] - open boxes and MIT/BATES [85] - open triangles. The solid and dashed curves correspond to the 'dressed' and 'bare' contributions from Ref. [86]; for R_{EM}, R_{SM}, only the 'dressed' contributions are shown; the 'bare' contributions are close to zero. The dotted curves are the predictions obtained in the large-N_c limit of QCD [87, 88].

crucial for the understanding of the nature of this state. There are several specific features in the extracted $\gamma^* p \to$ N(1440)P$_{11}$ amplitudes that are very important for testing models. First, this is the specific behavior of the transverse amplitude $A_{1/2}$, which being large and negative at $Q^2 = 0$, becomes large and positive at $Q^2 \simeq 2$ GeV^2, and then drops smoothly with Q^2. Second, the relative sign between the longitudinal $S_{1/2}$ and transverse $A_{1/2}$ amplitudes. And third, the common sign of the amplitudes $A_{1/2}, S_{1/2}$ extracted from the data on $\gamma^* p \to \pi N$ includes signs from the $\gamma^* p \to$ N(1440)P$_{11}$ and N(1440)P$_{11} \to \pi N$ vertices; both signs should be taken into account while comparing with model predictions. All these characteristics are described by the light-front relativistic quark models [95, 96] assuming that N(1440)P$_{11}$ is the first radial excitation of the $3q$ ground state. The presentation of the Roper resonance as a gluonic baryon excitation is definitely ruled out. No predictions exist for the $N\sigma$ molecule model.

3.6. The N(1535)S$_{11}$ state
For the first time the $\gamma^* N \to$ N(1535)S$_{11}$ transverse helicity amplitude has been extracted from the π electroproduction data in a wide range of Q^2 (Fig. 14), and the results confirm the Q^2-dependence of this amplitude observed in η electroproduction. Comparison of the results extracted from π and η photo- and electroproduction data have allowed to specify the relation between the branching ratios of N(1535)S$_{11}$ to the πN and ηN channels: from the fit to the amplitudes at $0 \leq Q^2 < 4.5$ GeV^2, we found

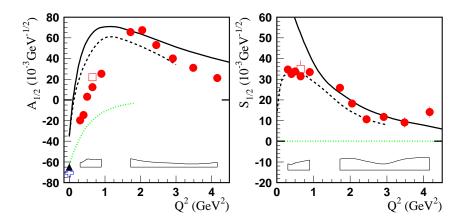$$\frac{\beta_{\eta N}}{\beta_{\pi N}} = 0.95 \pm 0.03. \tag{1}$$

Figure 13. Helicity amplitudes for the $\gamma^* p \to N(1440)P_{11}$ transition. The solid circles are the results extracted from the CLAS data [50, 51, 52, 53, 56, 57] in Ref. [63]. The bands show the model uncertainties. The cross at $Q^2 = 0$ is from SAID analysis that includes CLAS data on π^0 and π^+ photoproduction cross sections [30, 31]. The open boxes are obtained in the combined analysis of CLAS single π and 2π electroproduction data [66]. The full triangle at $Q^2 = 0$ is the RPP estimate [36]. All amplitudes, except RPP values, correspond to $M = 1440$ MeV, $\Gamma_{tot} = 350$ MeV, and $\beta_{\pi N} = 0.6$. The predictions of the LF relativistic quark models [95, 96] assuming $N(1440)P_{11}$ is a first radial excitation of the $3q$ ground state are shown by solid and dashed curves. The dotted curves are obtained assuming that the $N(1440)P_{11}$ is a gluonic baryon excitation (q^3G hybrid state) [92, 93].

Further, taking into account the branching ratio to the $\pi\pi N$ channel $\beta_{\pi\pi N} = 0.01 - 0.1$ [36], which accounts practically for all channels different from πN and ηN, we found

$$\beta_{\pi N} = 0.485 \pm 0.008 \pm 0.023, \tag{2}$$
$$\beta_{\eta N} = 0.460 \pm 0.008 \pm 0.022. \tag{3}$$

The first error corresponds to the fit error in Eq. (1) and the second error is related to the uncertainty of $\beta_{\pi\pi N}$. The obtained branching ratios (2,3) will enter into the 2010 edition of the RPP.

Due to the CLAS measurements of π electroproduction, for the first time the $\gamma^* N \to N(1535)S_{11}$ longitudinal helicity amplitude was extracted from experimental data. These results are crucial for testing theoretical models. It turned out that at $Q^2 < 3$ GeV^2, the sign of $S_{1/2}$ is not described by the quark models. Combined with the difficulties of quark models to describe the substantial coupling of $N(1535)S_{11}$ to the ηN channel [36] and to strange particles [99, 100], this can be indicative of a large meson-cloud contribution and(or) additional $q\bar{q}$ components in this state [101]. Alternative representations of the $N(1535)S_{11}$ as a meson-baryon molecule have been also discussed [102, 103, 104, 105].

3.7. The N(1520)D13 resonance
The CLAS data allowed the determination of the longitudinal amplitude of the $\gamma^* p \to N(1520)D_{13}$ transition, and much more accurate results are obtained for the transverse amplitudes (Fig. 15). There is a longstanding prediction of constituent quark models for the $\gamma^* p \to N(1520)D_{13}$ transition that follows from the structure of the nucleon and the $N(1520)D_{13}$ wave functions. It consists in the rapid helicity switch from the dominance of the $A_{3/2}$ amplitude at the photon point to the dominance of $A_{1/2}$ at $Q^2 > 1$ GeV^2. This prediction
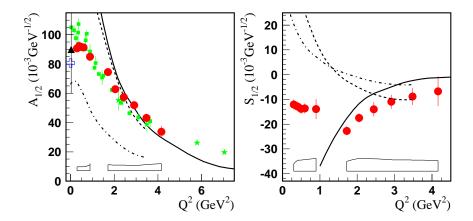
Figure 14. Helicity amplitudes for the $\gamma^* p \to$ N(1535)S$_{11}$ transition. The legend is partly as for Fig. 13. The solid boxes and stars are the CLAS [78, 79] and Hall C [80, 81] results, respectively, obtained in η electroproduction. All amplitudes, except RPP values, correspond to $M = 1535$ MeV, $\Gamma_{tot} = 150$ MeV, and to the branching ratios $\beta_{\pi N} = 0.485$, $\beta_{\eta N} = 0.46$ (2,3). The results of the LF relativistic quark models are given by the dashed [95] and dashed-dotted [97] curves. The solid curves show the amplitudes found within light-cone sum rules using lattice results for the light-cone distribution amplitudes of the N(1535)S$_{11}$ resonance [98].
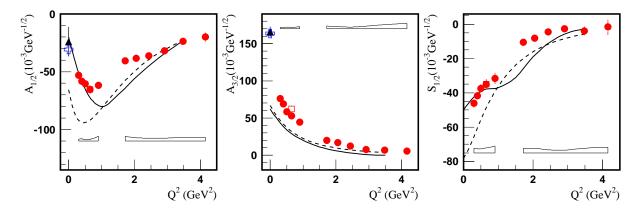

Figure 15. Helicity amplitudes for the $\gamma^* p \to$ N(1520)D$_{13}$ transition. The legend is partly as for Fig. 13. All amplitudes, except RPP values, correspond to $M = 1520$ MeV, $\Gamma_{tot} = 112$ MeV, and $\beta_{\pi N} = 0.6$. The curves correspond to the predictions of quark models: [106] (solid), [107] (dashed).

is definitely confirmed by the data, although quark models fail to describe the details of the Q^2 dependence of the amplitudes.

3.8. Transverse charge densities in the nucleon - resonance transitions

The accurate information now available for all amplitudes of the $\gamma^* p \to \Delta(1232)P_{33}$, N(1440)P$_{11}$, N(1520)D$_{13}$, and N(1535)S$_{11}$ transitions allowed, for the first time, to obtain spatial images of the transitions by mapping out the transition charge densities in impact parameter space. The corresponding result for the Roper resonance is presented in Fig. 16.
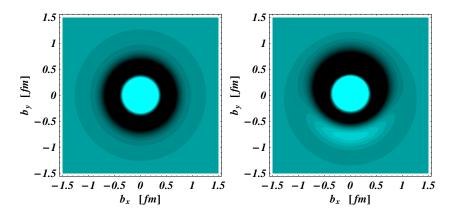
Figure 16. Quark transverse charge density in the $\gamma^* p \to$ N(1440)P$_{11}$ transition [108]. Left panel: unpolarized p and N(1440)P$_{11}$. Right panel: p and N(1440)P$_{11}$ polarized along the positive x-axis. The light (dark) areas are dominated by up (down) quarks and correspond to dominantly positive (negative) charges.

4. Excited Baryon Analysis Center

The Excited Baryon Analysis Center (EBAC) was established at JLab in January, 2006 to provide theoretical support to the excited baryon program. EBAC's program has two objectives. First, to establish the spectrum of excited nucleon states (N^*) and to extract the N^* parameters from the πN, γN and $N(e, e'\pi)$ data. The second objective is to develop theoretical interpretations of the extracted N^* parameters. To achieve these two goals, a dynamical coupled-channel reaction model (DCC) has been developed and is being used to perform analyses of the meson production data from JLab and other facilities. The essential feature of the DCC model is to account for the coupled-channel effects resulting from the unitarity conditions and the reaction mechanisms in the short range (off-shell) region where we want to map out the structure of baryons.

The DCC model is based on a Hamiltonian formulation [90] of multi-channel and multi-resonance reactions. The first work at EBAC was to determine the hadronic parameters of the model by fitting the world data on the $\pi N \to \pi N$, $\pi N \to \eta N$, and $\pi N \to \pi\pi N$ reactions. These were completed [109, 110, 111] with the results on the total πN cross sections shown in Fig. 17. The model was then applied to analyze pion photoproduction [112] and electroproduction [113] data. An important feature of the DCC model is the possibility to distinguish the N^* excitation due to the quark-gluon core from that due to the meson-cloud (meson-baryon dressing) effects. This is illustrated in Fig. 12 for the G_M^* form factor of the $\gamma N \to \Delta(1232)P_{33}$ transition. It is further found [86, 112] that the contribution due to the quark-gluon core is close to the prediction of constituent quark models.

In parallel, an exact analytic continuation method for extracting nucleon resonances from multi-channel reactions has been developed [114] and applied [115] to extract the nucleon resonances from this model. As an example, Fig. 18 shows the positions of the extracted P_{11} resonances in the complex energy plane. Within the DCC model, it is found that these two P_{11} resonances evolve from the same bare state with a mass of about 1700 MeV, which could be identified with the hadron structure calculations in the absence of meson-baryon degrees of freedom, such as the constituent quark model.

The plan at EBAC is to complete the analysis of single π and η production up to $W = 2$ GeV and $Q^2 \leq 6$ GeV^2, to analyze the 2π production data, and to extract the N^* form factors at the resonance poles. With these, EBAC will complete its first-stage analysis in 2010.
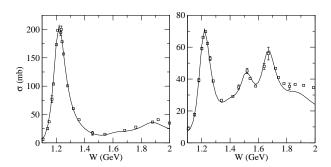
Figure 17. Total cross sections of $\pi^+ p$ (left) and $\pi^- p$ (right) reactions. The curves are from the dynamical coupled-channel model [109, 111].
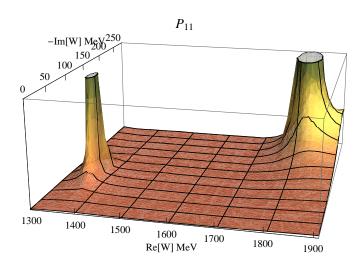

Figure 18. The P_{11} resonance poles extracted [114] from the dynamical coupled-channel model of Refs. [109, 111].

EBAC's second-stage work is to analyze the data of $K\Lambda$ and $K\Sigma$ production. EBAC is collaborating with the CLAS collaboration to develop methods for extracting $\gamma N \rightarrow K\Lambda$ multipole amplitudes as model independently as possible from the forthcoming JLab data from the over-complete measurements of $K\Lambda$ and $K\Sigma$ production.

Efforts are also being made to develop interpretations of the extracted N^* parameters in terms of hadron structure calculations. In addition to considering constituent quark models, we are also investigating how LQCD results can be related to the dynamical coupled-channel analysis [116].

5. Future prospects of the N^* program at 6 GeV and with the 12-GeV upgrade.

The main part of the experimental program to search for predicted new baryon states lies still in the future. The polarized frozen spin target facility FROST will be installed in CLAS in 2010 to complete the extensive program to measure double and triple polarization observables with protons that are polarized transversely to the production plane and to use linearly and circularly polarized photons. For the kaon-hyperon final states, the recoil polarization will be measured as well. Data taking with FROST will be followed with the equivalent program on

polarized neutrons. This part will use the polarized HD target and provide complementary information on the isospin content of the reaction and of the excited state. This information is required to separate isospin 1/2 from isospin 3/2 excitations. Moreover, selection rules allow the photo-excitation of some states, e.g. N(1675)D$_{15}$, from neutrons, but not from protons.

With the 12-GeV upgrade, the N^* program at JLab is being extended as an essential part of the comprehensive program of exclusive electroproduction measurements with the CLAS12 detector. A proposal for measuring π^0, η, and charged multi-pion final states in the unexplored domain of Q^2, from 5.0 to 12 GeV^2, has recently been approved by JLab's Program Advisory Committee of 2009.

The proposed experiments have three objectives [117]. The first is to map out the quark structure of N^*s from the data on exclusive meson electroproduction reactions. In the considered $Q^2 > 5.0$ GeV^2 domain, the meson-baryon dressing is weak, as illustrated in Fig. 12 for the $\Delta(1232)$P$_{33}$, and hence the extracted $\gamma^*N \to N^*$ form factors can be used more directly to probe the quark substructure of N^*s.

The second objective is to investigate the dynamics of dressed quark interactions inside the nucleon core and to understand how these interactions emerge from QCD. We are motivated by the recent advance in developing hadron models based on the Dyson-Schwinger equations (DSE) of QCD [118, 119], as well by exploratory attempts to evaluate transition γ^*NN^* from factors starting from QCD Lagrangian within the framework of LQCD [91, 98, 120, 121].

The third objective is to study the Q^2-dependence of the non-perturbative dynamics of QCD. This is based on the recent investigation of the momentum dependence of the dressed quark mass of the quark propagator within LQCD [122] and DSE [123]. Our focus is on the important question of how baryon structure emerges from confinement and dynamical chiral symmetry breaking of QCD.

The proposed experiments are closely related to the GPD program at JLab. The specification of exclusive reactions at high momentum transfer in terms of GPDs is a major goal of the CLAS12 upgrade. Experiments that are already approved as part of this program include deeply virtual Compton scattering and deeply virtual meson production.

References

[1] B. A. Mecking et al., Nucl. Inst. Meth. A **503**, 513, 2003.

[2] C. A. Keith et al., Nucl. Inst. Meth. A **501**, 327, 2003.

[3] R. Schumacher et al., Proposal: E-89-004 "Electromagnetic Production of Hyperons", 1989.

[4] B. Ritchie et al., Proposal: E-91-008 "Photoproduction of η, η' mesons", 1991.

[5] B. Ritchie et al., Proposal: E-94-008 "Photoproduction of η, η' mesons from deuterium", 1994.

[6] J. Ficenec et al., Proposal: E-94-103 "The photoproduction of pions", 1994.

[7] F. Klein et al., Proposal: E-99-013 "Photoproduction of omega mesons off protons with linearly polarized photons", 1999.

[8] F. Klein et al., Proposal: E-02-112 "Search for missing resonances in the photoproduction of hyperons using a polarized photon beam and a polarized target", 2002.

[9] S. Strauch et al., Proposal: E-03-105 "Pion photoproduction from a polarized target", 2003.

[10] E. Pasyuk et al., Proposal: E-05-012 "Measurements of polarization observables in eta-photoproduction with CLAS", 2005.

[11] V. Crede et al., Proposal: E-06-013 "Measurement of π^+, π^- photoproduction in double- polarization experiments using CLAS", 2006.

[12] P. Nadel-Turonski et al., Proposal: E-06-103 "Kaon production in the deuteron using polarized photons", 2006.

[13] V. Burkert et al., Proposal: E-89-037 "Electroproduction of the $P_{33}(1232)$ resonance", 1989.

[14] R. Minehart et al., Proposal: E-89-038 "Measurements of $p(e, e'\pi^+)n$, $p(e, e'p)\pi^0$, and $n(e, e'\pi^-)p$ in the second resonance region", 1989.

[15] S. Dytman et al., Proposal: E-89-039 "Amplitudes for the $S_{11}(1535)$ and $P_{11}(1710)$ resonances from an $ep \to e'p\eta$ experiment", 1989.

[16] V. Burkert et al., Proposal: E-89-042 "Measurement of the electron asymmetry in $p(e, e'\pi^+)n$ and $p(e, e'p)\pi^0$ in the mass region of the $P_{33}(1232)$", 1989.

[17] H. Funsten et al., Proposal: E-89-043 "Measurements of the electroproduction of the $\gamma^*(1520)$ and $f_0(975)$ via the K^+k^-p and $K^+\pi^-p$ final states", 1989.

[18] P. Stoler et al., Proposal: E-91-002 "The study of excited baryons at high momentum transfer with the CLAS spectrometer", 1991.

[19] R. Lourie et al., Proposal: E-91-011 "Recoil polarization measurements for neutral pion electroproduction at $Q^2 = 1$ GeV^2 near the Delta resonance", 1991.

[20] H. Funsten et al., Proposal: E-91-024 "Search for "missing" resonances in the electroproduction of ω mesons ", 1991.

[21] M. Ripani et al., Proposal: E-93-006 "Two pion decay of electroproduced baryon resonances", 1993.

[22] H. Weller et al., Proposal: E-93-036 "Measurement of of single pion electroproduction from the proton with polarized beam and polarized target using CLAS ", 1993.

[23] P. Stoler et al., Proposal: E-94-003 "Study of the $\Delta(1232)$ using double polarization asymmetries", 1994.

[24] P. Stoler et al., Proposal: E-94-014 "The $\Delta(1232)$ form factor at high momentum transfer", 1994.

[25] D. Carman et al., Proposal: E-99-006 "Polarization observables in the $p(e, e'K^\pm)\Lambda, \Sigma$ reaction", 1999.

[26] V. Burkert, P. Stoler et al., Proposal: E-99-107 "N^* excitations at high Q^2 in the $p\pi^0$, $n\pi^+$ channels", 1999.

[27] V. Burkert et al., Proposal: E-99-108 "N^* excitations at high Q^2 in the two-pion channel", 1999.

[28] D. Carman et al., Proposal: E-00-112 "Exclusive kaon electroproduction in Hall B at 6 GeV", 2000.

[29] P. Stoler et al., Proposal: E-01-002 "Baryon resonance electroproduction at high momentum transfer", 2001.

[30] M. Dugger et al., CLAS Collaboration, Phys. Rev. C **76**, 025211, 2007.

[31] M. Dugger et al., CLAS Collaboration, Phys. Rev. C **79**, 065206, 2009.

[32] M. Dugger et al., CLAS Collaboration, Phys. Rev. Lett. **89**, 222002, 2002, Erratum-ibid. **89**, 249904, 2002.

[33] M. Dugger et al., CLAS Collaboration, Phys. Rev. Lett. **96**, 062001, 2006, Erratum-ibid. **96**, 169905, 2006.

[34] J.W.C. McNabb et al., CLAS Collaboration, Phys. Rev. C **69**, 042201, 2004.

[35] R. Bradford et al., CLAS Collaboration, Phys. Rev. C **73**, 035202, 2006.

[36] C. Amsler *et al.* (*Review of Particle Physics*), Phys. Lett. B **667**, 1 (2008); http://pdg.lbl.gov/.

[37] G. Keaton and R. Workman, Phys. Rev. C **53**, 1434, 1996.

[38] R. Bradford et al., CLAS Collaboration, Phys. Rev. C **75**, 035205, 2007.

[39] V.A. Nikonov et al., Phys. Lett. B **662**, 245, 2008.

[40] E. Santopinto, Phys. Rev. C **72**, 022201, 2005.

[41] A. Lleres et al., GRAAL Collaboration, Eur. Phys. J. A **31**, 79, 2007.

[42] R. G. T. Zegers et al., LEPS Collaboration, Phys. Rev. Lett. **91**, 092001, 2003.

[43] A. Ramos et al., nucl-th/0502053, 2005.

[44] V. Burkert, Int. J. Mod. Phys. A **21**, 1764, 2006.

[45] R. De Vita et al., CLAS Collaboration, Phys. Rev. D **74**, 032001, 2006.

[46] M. Battaglieri et al., CLAS Collaboration, Phys. Rev. Lett. **96**, 042001, 2006.

[47] B. McKinnon et al., CLAS Collaboration, Phys. Rev. Lett. **96**, 212001, 2006.

[48] S. Niccolai et al., CLAS Collaboration, Phys. Rev. Lett. **97**, 032001, 2006.

[49] V. Kubarovski et al., CLAS Collaboration, Phys. Rev. Lett. 97, 102001, 2006.

[50] K. Joo et al., CLAS Collaboration, Phys. Rev. Lett. **88**, 122001 (2002).

[51] K. Joo et al., CLAS Collaboration, Phys. Rev. C **68**, 032201 (2003).

[52] K. Joo et al., CLAS Collaboration, Phys. Rev. C **70**, 042201 (2004).

[53] H. Egiyan et al., CLAS Collaboration, Phys. Rev. C **73**, 025204 (2006).

[54] M. Ungaro et al., CLAS Collaboration, Phys. Rev. Lett. **97**, 112003 (2006).

[55] L. C. Smith et al., CLAS Collaboration, Proceedings of the Workshop "Shape of Hadrons", p.222, Athens, 2006.

[56] K. Park et al., CLAS Collaboration, Phys. Rev. C **77**, 015208 (2008).

[57] A. Biselli et al., CLAS Collaboration, Phys. Rev. C **78**, 045204 (2008).

[58] G. F. Chew, M. L. Goldberger, F. E. Low, and Y. Nambu, Phys. Rev. **106**, 1345 (1957).

[59] S. Fubini, Y. Nambu, and V. Watagin, Phys. Rev. **111**, 329 (1958).

[60] I. G. Aznauryan, Phys. Rev. C **57**, 2727 (1998).

[61] I. G. Aznauryan, Phys. Rev. C **67**, 015209 (2003).

[62] I. G. Aznauryan et al., CLAS Collaboration, Phys. Rev. C **78**, 045209 (2008).

[63] I. G. Aznauryan et al., CLAS Collaboration, Phys. Rev. C **80**, 055203 (2009).

[64] D. Drechsel, O. Hanstein, S. Kamalov, and L. Tiator, Nucl. Phys. A **645**, 145 (1999).

[65] I. G. Aznauryan, V. D. Burkert, H. Egiyan, et al., Phys. Rev. C **71**, 015201 (2005).

[66] I. G. Aznauryan, V. D. Burkert, et al., Phys. Rev. C **72**, 045201 (2005).

[67] S. Capstick and W. Roberts, Prog. Part. Nucl. Phys., **45**, S241 (2000).

[68] S. Capstick and W. Roberts, Phys. Rev., D **49**, 4570 (1994).

[69] G. V. Fedotov et al., CLAS Collaboration, Phys. Rev. C **79**, 015204 (2009).

[70] M. Ripani et al., CLAS Collaboration, Phys. Rev. Lett. **91**, 022002 (2003).

[71] V. I. Mokeev et al., Phys. Rev. C **80**, 045212 (2009).

[72] V. I. Mokeev et al., Chinese Physics C **33**, 1210 (2009).

[73] V. I. Mokeev, Contributed talk at 12th International Conference on Meson-Nucleon Physics and the Structure of the Nucleon, May 31 -June 4, 2010, Williamsburg, VA, http://conferences.jlab.org/MENU10/program.html.

[74] J. J. Kelly, R. E. Roche, Z. Chai et al., Phys. Rev. Lett. **95**, 102001 (2005).

[75] J. J. Kelly, G. Gayou, R. E. Roche et al., Phys. Rev. C **75**, 025201 (2007).

[76] V. V. Frolov et al., Phys. Rev. Lett. **82**, 45 (1999).

[77] A.N. Villano et al., Phys. Rev. C **80**, 035203 (2009)

[78] R. Thompson et al., CLAS Collaboration, Phys. Rev. Lett. **86**, 1702 (2001).

[79] H. Denizli et al., CLAS Collaboration, Phys. Rev. C **76**, 015204 (2007).

[80] C. S. Armstrong et al., Phys. Rev. D **60**, 052004 (1999).

[81] M. M. Dalton et al., Phys. Rev. C **80**, 015205 (2009).

[82] W. W. Ash, Phys. Lett. B **24**, 165 (1967).

[83] S. Stave, M. O. Distler, I. Nakagawa et al., Eur. Phys. J. A **30**, 471 (2006).

[84] N. F. Sparveris, P. Achenbach, C. Ayerbe Gayoso et al., Phys. Lett. B **651**, 102 (2007).

[85] N. F. Sparveris, R. Alarcon, A. M. Bernstein et al., Phys. Rev. Lett. **94**, 022003 (2005).

[86] T. Sato and T.-S. H. Lee, Phys. Rev. C **63**, 055201 (2001).

[87] V. Pascalutsa, M. Vanderhaeghen, and S. N. Yang, Phys. Rep. **437**, 125 (2007).

[88] V. Pascalutsa and M. Vanderhaeghen, Phys. Rev. D **76**, 111501 (2007).

[89] S. Kamalov, S. N. Yang, D. Drechsel, O. Hanstein, and L. Tiator, Phys. Rev. C **64**, 032201 (2001).

[90] A. Matsuyama, T. Sato, and T.-S. H. Lee, Phys. Rep. **439**, 193 (2007).

[91] C. Alexandrou, G. Koutsou, H. Neff et al., Phys. Rev. D **77**, 085012 (2008).

[92] Z. P. Li, Phys. Rev. D **44**, 2841 (1991).

[93] Z. P. Li, V. Burkert, and Zh. Li, Phys. Rev. D **46**, 70 (1992).

[94] O. Krehl, et al., Phys. Rev. C **62**, 025207 (2000).

[95] S. Capstick and B. D. Keister, Phys. Rev. D **51**, 3598 (1995).

[96] I. G. Aznauryan, Phys. Rev. C **76**, 025212 (2007).

[97] E. Pace, G. Salmé, and S. Simula, Few Body Syst. Suppl. **10**, 407 (1999); E. Pace, G. Salmé, F. Cardarelli, and S. Simula, Nucl. Phys. A **666**, 33 (2000).

[98] V. M. Braun, M. Göckeler, R. Horsley et al., Phys. Rev. Lett. **103**, 072001 (2009).

[99] B. C. Liu and B. S. Zou, Phys. Rev. Lett. **96**, 142002 (2006).

[100] J. J. Xie, B. S. Zou, and H. C. Chiang, Phys. Rev. C **77**, 015206 (2008).

[101] C. S. An and B. S. Zou, arXiv:0802.3996 (nucl-th).

[102] N. Kaiser, P. B. Siegel, and W. Weise, Phys. Lett. B **362**, 23 (1995).

[103] J. Nieves and E. Riuz Arriola, Phys. Rev. D **64**, 116008 (2001).

[104] T. Inoue, E. Oset, and M. J. Vicente Vacas, Phys. Rev. C **65**, 035204 (2002).

[105] E. E. Kolomeitsev and M. F. M. Lutz, Phys. Lett. B **585**, 243 (2004).

[106] M. Warns, H. Schröder, W. Pfeil, and H. Rollnik, Z.Phys. C **45**, 627 (1990).

[107] M. Aiello, M. M. Giannini, and Santopinto, J.Phys. G **24**, 753 (1998).

[108] L. Tiator and M. Vanderhaeghen, Phys. Lett. B **672**, 344 (2009).

[109] B. Julia-Diaz, T.-S. H. Lee, A. Matsuyama, and T. Sato, Phys. Rev. C **76**, 065201 (2007).

[110] J. Durand, B. Julia-Diaz, T.-S. H. Lee, B. Saghai, and T. Sato, Phys. Rev. C **78**, 025204 (2008).

[111] H. Kamano, B. Julia-Diaz, T.-S. H. Lee, A. Matsuyama, and T. Sato, Phys. Rev. C **79**, 025206 (2009).

[112] B. Julia-Diaz, T.-S. H. Lee, A. Matsuyama, T. Sato, and L.C. Smith, Phys. Rev. C **77**, 045205 (2008).

[113] B. Julia-Diaz, H. Kamano, T.-S. H. Lee, A. Matsuyama, T. Sato, and N. Suzuki, in preparation.

[114] N. Suzuki, T. Sato, and T.-S. H. Lee, Phys. Rev. C **79**, 025205 (2009).

[115] N. Suzuki, B. Julia-Diaz, H. Kamano, T.-S. H. Lee, A. Matsuyama, and T. Sato, in preparation.

[116] R. Young and T.-S. H. Lee, in preparation.

[117] I.Aznauryan et al., Theory Support for the Excited Baryon Program at the Jlab 12-GeV Upgrade, arXiv:0707.1901 [nucl-th].

[118] A. Höll, *et al.*, Phys. Rev. C **71**, 065204 (2005).

[119] G. Eichmann, R. Alkofer, I. C. Cloët, A. Krassnigg and C. D. Roberts, Phys. Rev. C **77** (2008) 042202(R).

[120] C. Alexandrou, arXiv:09064137, hep-lat, Invited talk at the Workshop on the Physics of excited nucleons NSTAR2009, Beijing, April 2009

[121] H.-W. Lin, S.D. Cohen, R.G. Edvards, and D.G. Richards, Phys. Rev. D **78**, 114508 (2008)

[122] P.O. Bownman et al, Phys. Rev. C **71**, 0454507 (2005).

[123] M.S. Bhagwat, M.A. Pichowsky, C.D. Roberts, P.C. Tandy, Phys. Rev. C **68** (2003).